Hindawi
International Journal of Antennas and Propagation
Volume 2018, Article ID 1963051, 7 pages
https://doi.org/10.1155/2018/1963051

Research Article

Frequency-Tunable Electromagnetic Absorber by Mechanically Controlling Substrate Thickness

Heijun Jeong,[1] Manos M. Tentzeris,[2] and Sungjoon Lim[1]

[1]*School of Electrical and Electronics Engineering, College of Engineering, Chung-Ang University, Seoul 156-756, Republic of Korea*
[2]*School of Electrical and Computer Engineering, Georgia Institute of Technology, Atlanta, GA 30332-0250, USA*

Correspondence should be addressed to Manos M. Tentzeris; etentze@ece.gatech.edu and Sungjoon Lim; sungjoon@cau.ac.kr

Received 19 March 2018; Accepted 28 May 2018; Published 29 August 2018

Academic Editor: Atsushi Mase

In this paper, we propose a frequency-tunable electromagnetic absorber that uses the mechanical control of substrate thickness. The absorption frequency of the proposed absorber can be changed by varying the substrate thickness. In order to mechanically control the substrate thickness, we introduce a 3D-printed molding with air space. The proposed structure consists of two layers and one frame: the FR4 substrate, polylactic acid (PLA) frame, and air substrate. The FR4 and PLA thicknesses are fixed, and the air thickness is varied using the PLA frame. Therefore, the effective dielectric constant of the overall substrate can be changed. The metallic rectangular patch and ground are patterned on the top and bottom FR4 substrates, respectively. The performance of the proposed tunable absorber is demonstrated from full-wave simulation and measurements. When both of the FR4 substrate thicknesses are 0.3 mm and the air thickness is changed from 1 to 3.5 mm, the absorption frequency is changed from 8.9 to 8.0 GHz, respectively. Therefore, the frequency-tuning capability of the proposed absorber is successfully demonstrated.

1. Introduction

Metamaterials are artificial structures in which periodic unit cells are infinitely arranged. Using these metamaterials, we can control the characteristics of a material [1]. These technologies are used in various fields, such as stealth technology [2, 3], electromagnetic interference (EMI) and electromagnetic compatibility (EMC) solutions [4], superlenses [5, 6], RF circuit applications [7], and sound wave technology [8]. Metamaterial absorbers are also one of its promising applications. The metamaterial absorber was first proposed by Landy et al. [9]. The previous absorbers, such as ferrite [10–13] or wedge-tapered [14, 15] absorbers, were bulky and, therefore, were limited by space. Compared to material-based electromagnetic (EM) absorbers, structure-based metamaterial absorbers show high absorption rates, low production costs, and functionality with a low profile.

In spite of the several advantages of the metamaterial absorber, it has the disadvantage of a narrow bandwidth, because it uses electromagnetic resonance. Therefore, in order to overcome this disadvantage, metamaterial absorbers have been designed using lossy patterns [16–18], multiresonance [19–21], and lumped components [22–24], in order to broaden the absorption frequencies. A frequency-tunable metamaterial absorber is an alternative solution. The frequency-tunable metamaterial absorber can be used not only as an electromagnetic absorber but also as a frequency-selective sensor. Most frequency-tunable metamaterial absorbers have been realized using electronic devices such as diodes [25–27], microelectromechanical systems (MEMS) [28–30], and liquid crystal technology [31, 32]. Recently, fluidically tunable metamaterial absorbers have been proposed using liquid metal [33–35]. These electrically tunable devices show an instantaneous response. However, they are not only costly but also have limitations of design in a periodic structure because of additional DC bias lines and an extremely large number of devices. Alternatively, frequency-tunable metamaterial absorbers using liquid crystal or liquid metal can be fabricated not only on hard substrates but also on flexible substrates. In spite of its slow

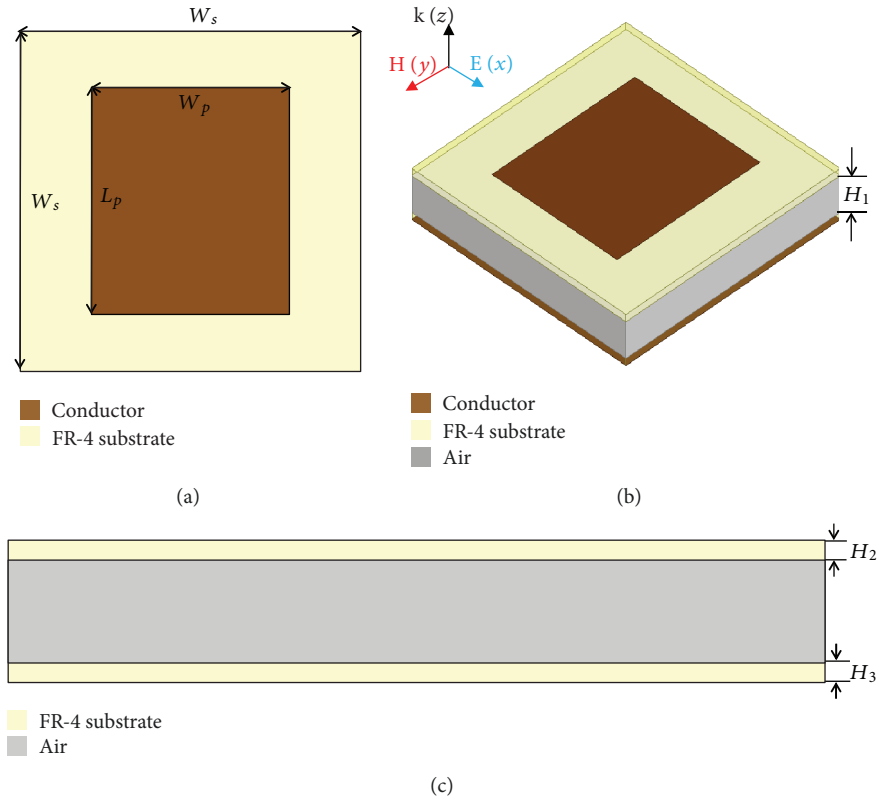

FIGURE 1: Geometry of the unit cell of the proposed absorber. (a) Top view of the unit cell. (b) Perspective view of the unit cell. (c) Side view of the unit cell. $W_s = 12$ mm; $L_p = 8$ mm; $W_p = 7$ mm; $H_1 = 1.5$ mm; $H_2 = H_3 = 0.5$ mm.

tuning speed, this type of tunable absorbers has drawn interest due to its flexibility and simple design.

Recently, mechanically tunable metamaterial absorbers have been proposed using stretching technology [36–38]. For instance, the physical size of the unit cell can be deformed by stretching the substrate. Its tuning speed is slow, but it has a simple design and low cost for a periodic structure. Because the absorption frequency can be determined by the deformation level, a mechanically tunable absorber can be used for frequency tunability as well as physical strain sensors.

In this paper, we proposed a novel frequency-tunable EM absorber by mechanically controlling the substrate thickness. The proposed thickness-controllable substrate consists of the FR4 layer with fixed thickness and the air layer with controllable thickness. In order to mechanically control the thickness of the substrate, a polylactic acid (PLA) frame using a 3D printer was fabricated. The frequency tunability of the proposed EM absorber is successfully demonstrated through full-wave simulation and measurement.

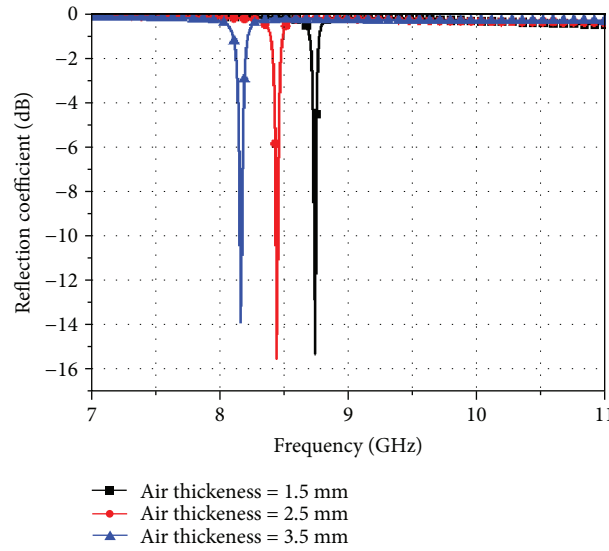

FIGURE 2: Simulated reflection coefficients of the proposed absorber at different air thicknesses.

2. Electromagnetic Absorber Design

In this paper, we proposed a rectangular patch for the unit cell of the absorber. Figure 1 shows the geometry of a unit cell of the proposed absorber with geometrical dimensions. The unit cell size ($Ws \times Ws$) is 12 mm × 12 mm. The proposed absorber is composed of two FR-4 substrates with the air substrate in between, as illustrated in Figure 1(b). The dielectric constant and tangent loss of the FR-4 substrate are 4.4 and 0.02, respectively. The patch is designed on the top of the upper FR-4 substrate. The ground plane is designed on the bottom FR-4 substrate. Both FR-4 substrates have a fixed thickness (H_2 and H_3) of 0.5 mm. The air substrate thickness (H_1) can be varied from 1.5 mm to 3.5 mm. In this work, the patch size is fixed, and the substrate thickness

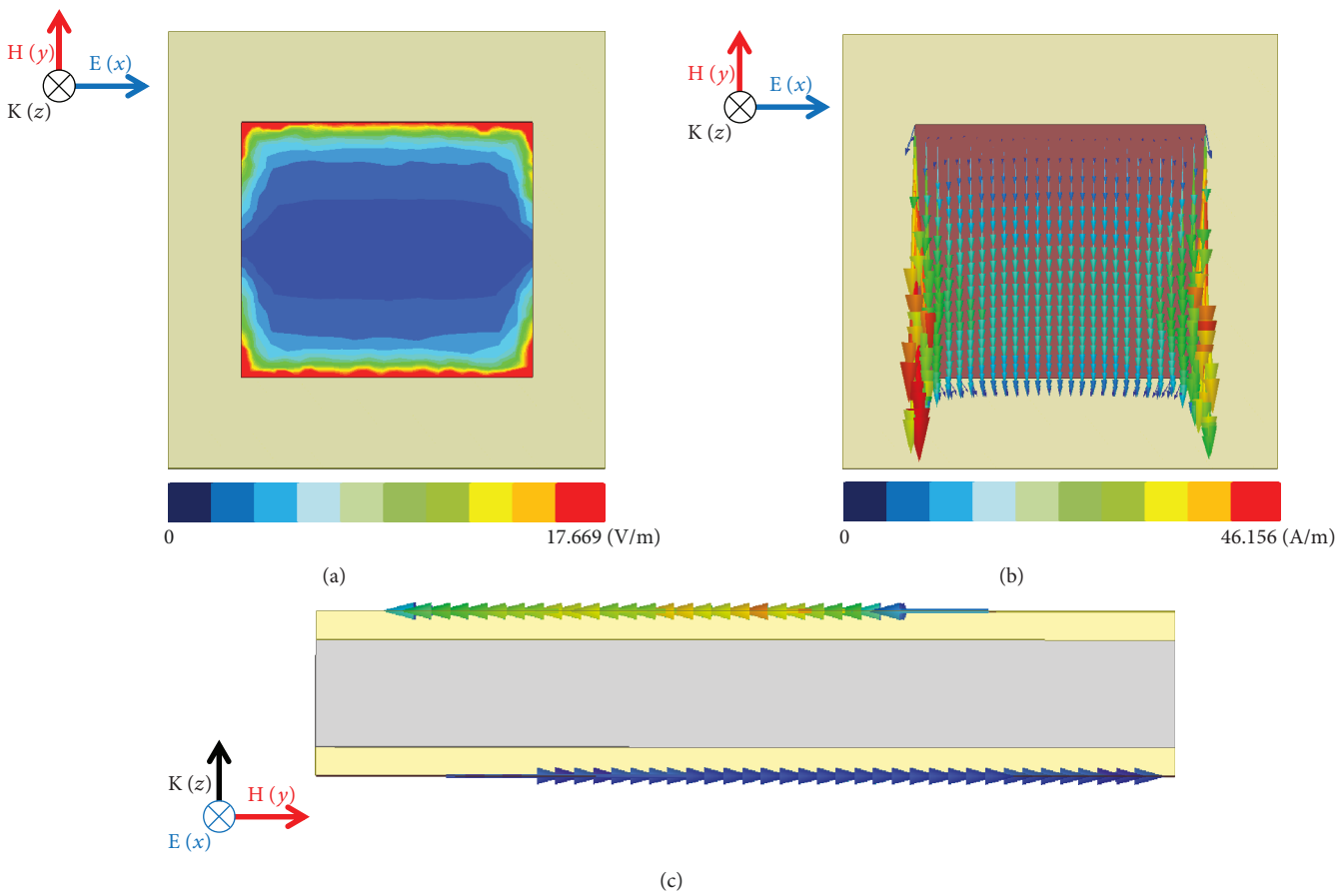

Figure 3: (a) Simulated electric field distribution; (b) top and (c) side view of the vector current density of the proposed absorber.

is varied. In particular, when the thickness of the air substrate is varied, H_s and ε_{eff} are changed, thereby changing the resonant frequency.

3. Simulation Results

Figure 2 shows the simulated reflection coefficients of the proposed absorber at different air thickness of 1.5 mm, 2.5 mm, and 3.5 mm. ANSYS high-frequency structure simulator (HFSS) is used for full-wave analysis. It is observed that the resonant frequency is 8.7 GHz with a reflection coefficient of −15 dB when the air thickness is 1.5 mm. When the thickness of the air layer is increased to 2.5 mm and 3.5 mm, the resonant frequency decreased to 8.4 GHz and 8.2 GHz, respectively. Therefore, the resonance frequency shifted by 0.5 GHz from 8.7 to 8.2 GHz. Figure 3 shows the simulation results of the electrical field distribution and vector current density of the proposed absorber when the E- and H-fields are incident on x and y polarization, respectively.

As shown in Figure 3(a), the electrical field is distributed on an edge of the patch along the x direction, which generates an electric response. The vector current density flows in the y direction, as shown in Figure 3(b). The top and bottom planes of the vector current densities flow in the $+y$ and $-y$ direction, which generates a magnetic response as shown in Figure 3(c).

4. Measurement Results

For the experiment, we used a monostatic RCS measurement setup. Figure 4 shows the illustration of the monostatic far-field RCS measurement system. After the prototype is fabricated, we measured the reflection coefficient to prove the performance. The absorption is calculated by (1). Because the bottom is covered entirely by copper, there is no transmitted wave (T). Therefore, the absorption is calculated only from the reflection coefficient (Γ).

$$A(\omega) = 1 - \Gamma(\omega) - T(\omega) = 1 - \Gamma(\omega). \quad (1)$$

To measure the reflection coefficient of the prototype, we used a single WR-90 PE9856/SF-15 horn antenna (Pasternack, CA, USA). The operating frequency range is 8.2–12.4 GHz, and the nominal gain is 15 dB. The antenna far field for measurement is 0.5 meter. The back side of the prototype is placed in the wedge-tapered absorber, which prevents unexpected reflected waves. We analyzed the experiment results using an Anritsu MS2038C vector network analyzer, utilizing the time-gating function for measurement.

Figure 5 shows the 3D-printed frame for the fixed air thickness. As shown in Figure 5(a), we fabricated a PLA frame with 0.5 mm interval slots. We used the Ultimaker2+ 3D printer (Ultimaker B.V., Geldermalsen, Netherlands) for the PLA frame fabrication. Figure 5(b) shows a picture

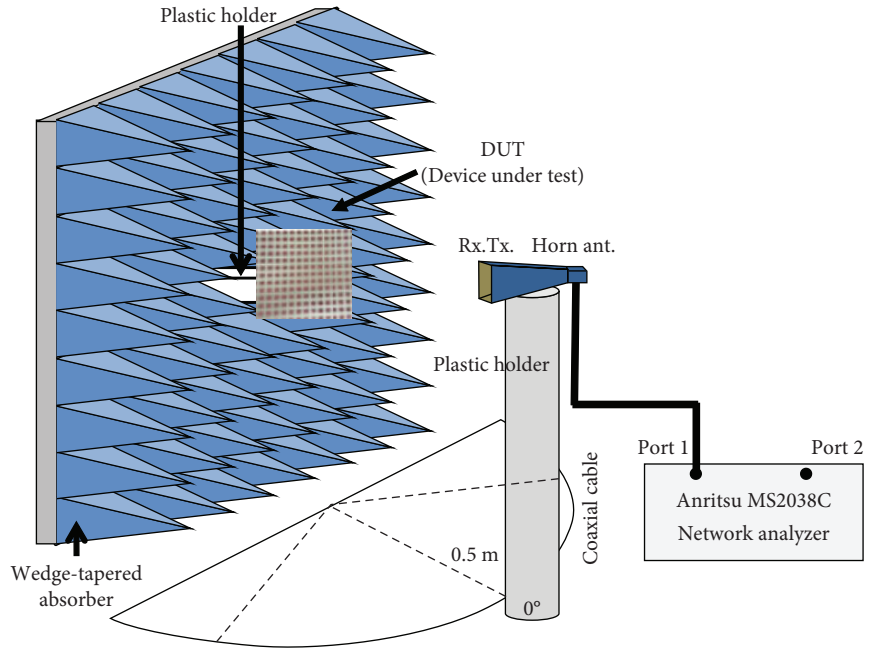

Figure 4: Illustration of the free space absorption ratio measurement setup under normal incidence.

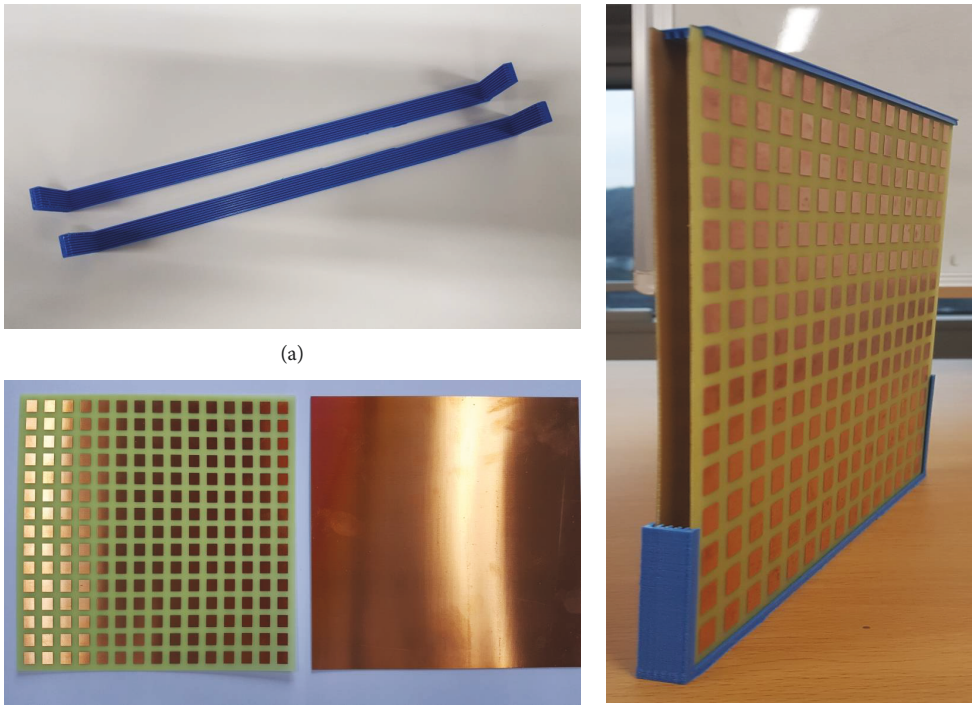

Figure 5: Pictures of the 3D-printed frame for the fixed air thickness. (a) Fabricated 3D PLA frame. (b) The fabricated absorber. (c) 3D PLA frame with an absorber.

of a fabricated absorber. The fabricated absorber size is 180 mm × 180 mm. Figure 5(c) shows the combined PLA frame and absorber.

Figure 6 shows the measured reflection coefficient according to the change in air thickness and the relation between the measurement results and fitted curve. In Figure 6(a), when the air layer thickness is 1.5 mm, the resonant frequency is 8.9 GHz with −41 dB. When the thickness of the air layer was increased from 1.5 mm to 2.5 mm and 3.5 mm, respectively, the resonant frequencies decreased from 8.9 GHz to 8.5 GHz and 8.0 GHz. Figure 6(b) shows the relation between the measurement results and fitted

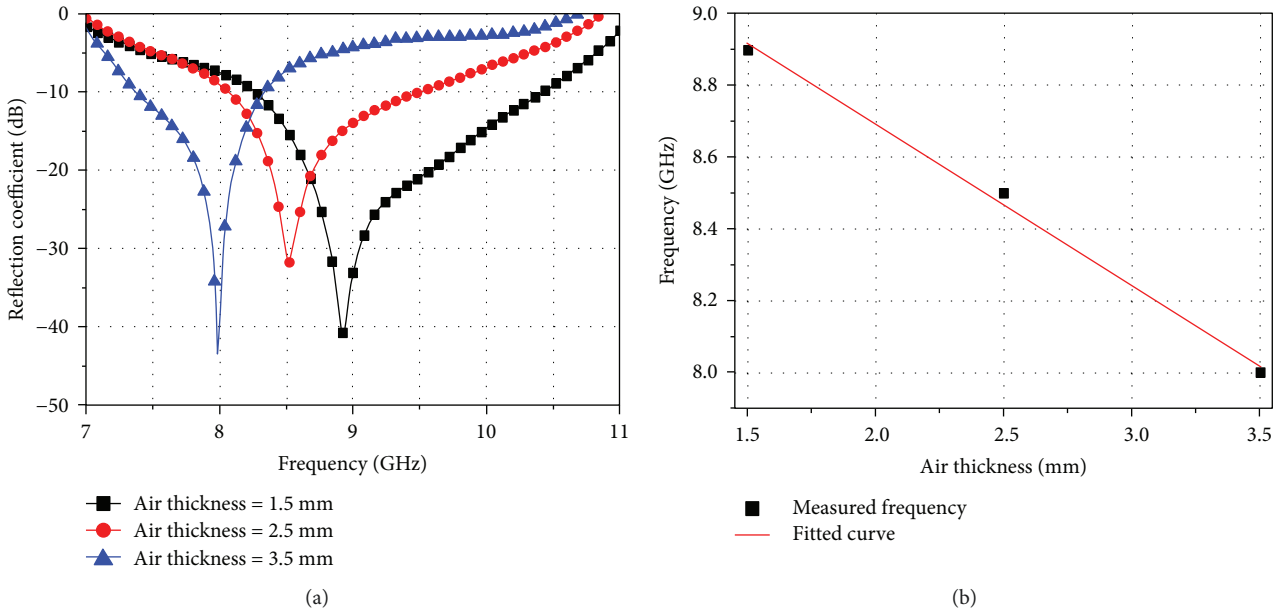

Figure 6: Measured reflection coefficient according to change in air thickness and the relation between the measurement results and fitted curve.

Table 1: Comparison of the proposed mechanically frequency reconfigurable absorber with those of other papers.

Reference paper	Tuning method	Tuning frequency range (GHz)	BW* (%)
[38]	Mechanically stretchable	11.15–11.56	3
[39]	Mechanically stretchable	640–680	8
[40]	Microelectromechanical system (MEMS)	1280–1320	3
[37]	Mechanically stretchable	10.4–11.0	5
Proposed work	Mechanically control the substrate thickness	8.0–8.9	10

*$BW = \Delta f / f_c$, where $\Delta f = f_{high} - f_{low}$ and $f_c = (f_{high} + f_{low})/2$.

curve. From the fitted curve of $y = -0.45x + 9.519$, the sensitivity is defined to be 4.5×10^8 Hz/mm when the air layer thickness is changed. Table 1 shows the comparison between the proposed work and other papers. The proposed work shows wider tuning range and bandwidth compared to other works.

5. Conclusions

In this paper, we proposed frequency-tunable electromagnetic absorber using the mechanical control of substrate thickness. In order to control the substrate thickness, a PLA frame fabricated with a 3D printer was used as the fixed substrate thickness, mechanically. We used two FR4 substrates with a middle air layer to control the thickness of the air layer mechanically. The top side of the upper substrate is designed by patch. The bottom side of the bottom substrate is designed as ground. The patch dimension of a unit cell is 8 mm × 7 mm, and the overall fabricated absorber is 180 mm × 180 mm. To perform the measurement, we set up a monostatic RCS measurement. The measurement was performed using a WR-90 horn antenna and a network analyzer. The resonant frequency was matched to 8.9 GHz with a reflection coefficient of −41 dB. When the air thickness increased from 1.5 mm to 2.5 mm and 3.5 mm, the resonant frequency decreased from 8.9 GHz to 8.5 GHz and 8.0 GHz, respectively, shifted by up to 0.9 GHz. Therefore, we proved the successful fabrication of a frequency-tunable electromagnetic absorber using a mechanically controlled substrate thickness and proved the results through simulation and measurement.

Data Availability

The structures are simulated and analyzed by ANSYS HFSS (high-frequency structure simulator).

Conflicts of Interest

The authors declare that there is no conflict of interest regarding the publication of this paper.

Acknowledgments

This research was supported in part by Chung-Ang University Research Grants in 2018 and in part by the National Research Foundation of Korea (NRF) grant

funded by the Korean government (MSIP) (no. 2017R1A2B3003856).

References

[1] C. M. Watts, X. L. Liu, and W. J. Padilla, "Metamaterial electromagnetic wave absorbers," *Advanced Materials*, vol. 24, no. 23, pp. OP98–OP120, 2012.

[2] D. Schurig, J. J. Mock, B. J. Justice et al., "Metamaterial electromagnetic cloak at microwave frequencies," *Science*, vol. 314, no. 5801, pp. 977–980, 2006.

[3] K. Iwaszczuk, A. C. Strikwerda, K. Fan, X. Zhang, R. D. Averitt, and P. U. Jepsen, "Flexible metamaterial absorbers for stealth applications at terahertz frequencies," *Optics Express*, vol. 20, no. 1, pp. 635–643, 2012.

[4] S. Shahparnia and O. M. M. Ramahi, "Electromagnetic interference (EMI) reduction from printed circuit boards (PCB) using electromagnetic bandgap structures," *IEEE Transactions on Electromagnetic Compatibility*, vol. 46, no. 4, pp. 580–587, 2004.

[5] N. Fang, H. Lee, C. Sun, and X. Zhang, "Sub–diffraction-limited optical imaging with a silver superlens," *Science*, vol. 308, no. 5721, pp. 534–537, 2005.

[6] K. Aydin, I. Bulu, and E. Ozbay, "Subwavelength resolution with a negative-index metamaterial superlens," *Applied Physics Letters*, vol. 90, no. 25, article 254102, 2007.

[7] D.-S. Eom and H.-Y. Lee, "A broadband half-mode substrate integrated waveguide quadrature Wilkinson power divider using composite right/left-handed transmission line," *Journal of Electromagnetic Engineering and Science*, vol. 17, no. 1, pp. 9–13, 2017.

[8] Z. Yang, H. M. Dai, N. H. Chan, G. C. Ma, and P. Sheng, "Acoustic metamaterial panels for sound attenuation in the 50–1000 Hz regime," *Applied Physics Letters*, vol. 96, no. 4, article 041906, 2010.

[9] N. I. Landy, S. Sajuyigbe, J. J. Mock, D. R. Smith, and W. J. Padilla, "Perfect metamaterial absorber," *Physical Review Letters*, vol. 100, no. 20, article 207402, 2008.

[10] M.-J. Park, J. Choi, and S.-S. Kim, "Wide bandwidth pyramidal absorbers of granular ferrite and carbonyl iron powders," *IEEE Transactions on Magnetics*, vol. 36, no. 5, pp. 3272–3274, 2000.

[11] J. Y. Shin and J. H. Oh, "The microwave absorbing phenomena of ferrite microwave absorbers," *IEEE Transactions on Magnetics*, vol. 29, no. 6, pp. 3437–3439, 1993.

[12] K. Hatakeyama and T. Inui, "Electromagnetic wave absorber using ferrite absorbing material dispersed with short metal fibers," *IEEE Transactions on Magnetics*, vol. 20, no. 5, pp. 1261–1263, 1984.

[13] D.-Y. Kim, Y.-H. Yoon, K.-J. Jo, G.-B. Jung, and C.-C. An, "Effects of sheet thickness on the electromagnetic wave absorbing characterization of $Li_{0.375}Ni_{0.375}Zn_{0.25}$-ferrite composite as a radiation absorbent material," *Journal of Electromagnetic Engineering and Science*, vol. 16, no. 3, pp. 150–158, 2016.

[14] J. W. Head, "The design of gradual transition (wedge) absorbers for a free-field room," *British Journal of Applied Physics*, vol. 16, no. 7, pp. 1009–1014, 1965.

[15] C. L. Holloway and E. F. Kuester, "A low-frequency model for wedge or pyramid absorber arrays-II: computed and measured results," *IEEE Transactions on Electromagnetic Compatibility*, vol. 36, no. 4, pp. 307–313, 1994.

[16] H.-B. Zhang, P.-H. Zhou, H.-P. Lu, Y.-Q. Xu, D.-F. Liang, and L.-J. Deng, "Resistance selection of high impedance surface absorbers for perfect and broadband absorption," *IEEE Transactions on Antennas and Propagation*, vol. 61, no. 2, pp. 976–979, 2013.

[17] F. A. Costa and A. Monorchio, "A frequency selective radome with wideband absorbing properties," *IEEE Transactions on Antennas and Propagation*, vol. 60, no. 6, pp. 2740–2747, 2012.

[18] J. Lee and B. Lee, "Design of thin RC absorbers using a silver nanowire resistive screen," *Journal of Electromagnetic Engineering and Science*, vol. 16, no. 2, pp. 106–111, 2016.

[19] H. Luo, X. Hu, Y. Qiu, and P. Zhou, "Design of a wide-band nearly perfect absorber based on multi-resonance with square patch," *Solid State Communications*, vol. 188, pp. 5–11, 2014.

[20] J. W. Park, P. van Tuong, J. Y. Rhee et al., "Multi-band metamaterial absorber based on the arrangement of donut-type resonators," *Optics Express*, vol. 21, no. 8, pp. 9691–9702, 2013.

[21] X. Y. Peng, B. Wang, S. Lai, D. H. Zhang, and J. H. Teng, "Ultrathin multi-band planar metamaterial absorber based on standing wave resonances," *Optics Express*, vol. 20, no. 25, pp. 27756–27765, 2012.

[22] C. Mias and J. H. Yap, "A varactor-tunable high impedance surface with a resistive-lumped-element biasing grid," *IEEE Transactions on Antennas and Propagation*, vol. 55, no. 7, pp. 1955–1962, 2007.

[23] F. Costa, A. Monorchio, and G. Manara, "Analysis and design of ultra thin electromagnetic absorbers comprising resistively loaded high impedance surfaces," *IEEE Transactions on Antennas and Propagation*, vol. 58, no. 5, pp. 1551–1558, 2010.

[24] Y. Z. Cheng, Y. Wang, Y. Nie, R. Z. Gong, X. Xiong, and X. Wang, "Design, fabrication and measurement of a broadband polarization-insensitive metamaterial absorber based on lumped elements," *Journal of Applied Physics*, vol. 111, no. 4, article 044902, 2012.

[25] A. Tennant and B. Chambers, "Adaptive radar absorbing structure with PIN diode controlled active frequency selective surface," *Smart Materials and Structures*, vol. 13, no. 1, pp. 122–125, 2004.

[26] W. Xu and S. Sonkusale, "Microwave diode switchable metamaterial reflector/absorber," *Applied Physics Letters*, vol. 103, no. 3, article 031902, 2013.

[27] A. Tennant and B. Chambers, "A single-layer tuneable microwave absorber using an active FSS," *IEEE Microwave and Wireless Components Letters*, vol. 14, no. 1, pp. 46-47, 2004.

[28] H. Tao, A. C. Strikwerda, K. Fan, W. J. Padilla, X. Zhang, and R. D. Averitt, "MEMS based structurally tunable metamaterials at terahertz frequencies," *Journal of Infrared, Millimeter, and Terahertz Waves*, vol. 32, no. 5, pp. 580–595, 2011.

[29] H. Bilgin, S. Zahertar, S. Sadeghzadeh, A. D. Yalcinkaya, and H. Torun, "A MEMS-based terahertz detector with metamaterial-based absorber and optical interferometric readout," *Sensors and Actuators A: Physical*, vol. 244, no. 15, pp. 292–298, 2016.

[30] T. Y. Li, L. Wang, J. M. Wang, S. Li, and X. J. He, "A dual band polarization-insensitive tunable absorber based on terahertz MEMS metamaterial," *Integrated Ferroelectrics*, vol. 151, no. 1, pp. 157–163, 2014.

[31] G. Isić, B. Vasić, D. C. Zografopoulos, R. Beccherelli, and R. Gajić, "Electrically tunable critically coupled terahertz metamaterial absorber based on nematic liquid crystals," *Physical Review Applied*, vol. 3, no. 6, article 064007, 2015.

[32] D. Shrekenhamer, W. C. Chen, and W. J. Padilla, "Liquid crystal tunable metamaterial absorber," *Physical Review Letters*, vol. 110, no. 17, article 177403, 2013.

[33] K. Ling, H. Kim, M. Yoo, and S. Lim, "Frequency-switchable metamaterial absorber injecting eutectic gallium-indium (EGaIn) liquid metal alloy," *Sensors*, vol. 15, no. 11, pp. 28154–28165, 2015.

[34] K. Kim, D. Lee, S. Eom, and S. Lim, "Stretchable metamaterial absorber using liquid metal-filled polydimethylsiloxane (PDMS)," *Sensors*, vol. 16, no. 4, p. 521, 2016.

[35] H. K. Kim, D. Lee, and S. Lim, "Wideband-switchable metamaterial absorber using injected liquid metal," *Scientific Reports*, vol. 6, no. 1, article 31823, 2016.

[36] S. Yang, P. Liu, M. Yang, Q. Wang, J. Song, and L. Dong, "From flexible and stretchable meta-atom to metamaterial : a wearable microwave meta-skin with tunable frequency selective and cloaking effects," *Scientific Reports*, vol. 6, no. 1, pp. 21921–21929, 2016.

[37] H. Jeong and S. Lim, "A stretchable electromagnetic absorber fabricated using screen printing technology," *Sensors*, vol. 17, no. 5, pp. 1175–1184, 2017.

[38] F. Zhang, S. Feng, K. Qiu et al., "Mechanically stretchable and tunable metamaterial absorber," *Applied Physics Letters*, vol. 106, no. 9, article 091907, 2015.

[39] J. Li, C. M. Shah, W. Withayachumnankul et al., "Mechanically tunable terahertz metamaterials," *Applied Physics Letters*, vol. 102, no. 12, article 121101, 2013.

[40] F. Hu, Y. Qian, Z. Li et al., "Design of a tunable terahertz narrowband metamaterial absorber based on an electrostatically actuated MEMS cantilever and split ring resonator array," *Journal of Optics*, vol. 15, no. 5, article 055101, 2013.